

Vibrational Smearing of Deformation Densities in Diatomic Molecules. An Application of Hartree–Fock–Slater SCF Calculations

BY A. ROZENDAAL AND P. ROS

Scheikundig Laboratorium der Vrije Universiteit, De Boelelaan 1083, 1081 HV Amsterdam, The Netherlands

(Received 7 April 1981; accepted 22 January 1982)

Abstract

The smearing of the deformation density in the diatomics H_2 , CH, BeH, CO and N_2 , caused by internal vibration, is calculated using a large number of LCAO Hartree–Fock–Slater electronic wavefunctions. Both the effect of anharmonicity and the thermal population of rotational and vibrational states at 300 K are considered. The main conclusion is that the effect of the smearing is very small for these molecules. Compared to the effect of the anharmonic zero-point vibration upon the charge deformation density, the influence of including higher states at 300 K is negligible.

Introduction

Comparison of experimental charge density distribution with theoretical densities in molecules is a complicated subject, partly due to the difference caused by nuclear motions included in the former, and the usual static approach (Born–Oppenheimer approximation) of the latter (Feil, 1977; Hirshfeld, 1977). A reliable comparison demands a deconvolution of experimental densities (Fink, Gregory & Moore, 1976; Hirshfeld, 1976) or a convolution of the theoretically calculated densities. Stevens, Rys & Coppens (1977) argue the latter approach to be more desirable, which will be discussed in the present study too.

The complexity of the nuclear motions in a molecule or molecular crystal requires a number of approximations in a theoretical treatment. These motions are often supposed to be separable into non-coupling internal motions and external or rigid-body motions. The latter have in most systems much larger amplitudes. With this distinction, the smearing of the electron density due to external modes can be studied using a convolution of the internal charge density distribution onto a probability function describing the rigid-body motions (Hirshfeld, 1977; Coppens & Stevens, 1977; Stevens *et al.*, 1977; Coulson & Thomas, 1971; Thomas, 1973). It is this internal charge density, or more precisely the deformation density, which we will consider in detail.

The usual starting point for calculation of the charge density is the spin-restricted electronic wavefunction. This function, and hence the charge density, is in the Born–Oppenheimer approximation parametrically dependent on the nuclear coordinates \mathbf{R} (Smith & Absar, 1977; Stewart, 1977). The time-averaged internal density $\rho_{\text{int}}(\mathbf{r})$ is then found from the canonical ensemble average over the states n for the nuclear wavefunction $\psi_n(\mathbf{R})$ (Stewart, 1977; Epstein & Stewart, 1979):

$$\rho_{\text{int}}(\mathbf{r}) = \sum_n W_n \int \psi_n^*(\mathbf{R}) \rho(\mathbf{r}; \mathbf{R}) \psi_n(\mathbf{R}) d\mathbf{R},$$

for short,

$$\rho_{\text{int}}(\mathbf{r}) = \sum_n W_n I_n(\mathbf{r}), \quad (1)$$

where W_n are temperature-dependent normalized Boltzmann factors. Evaluation of (1) demands in principle an infinite number of electronic wavefunctions with different values of \mathbf{R} . This will give rise to further approximations.

Previous studies concerning approximate solutions of (1) are ultimately restricted to the harmonic or anharmonic zero-point vibration. For example, we mention the attack on this problem by Coulson & Thomas (1971), who used a convolution of only the molecular charge density at equilibrium distance onto the square of the vibrational wavefunction. Ruysink & Vos (1974) extended this approach with averaged normalization factors of the molecular orbitals. Becker (1977) showed results obtained with a numerical integration technique, using many electronic wavefunctions. Stewart (1977) and Epstein & Stewart (1979) studied the vibrational average of X-ray scattering intensities and diatomic molecular form factors, using a rigid pseudo-atom approximation. The effect of non-rigid terms in a pseudo-atom approximation was also studied by Epstein & Stewart (1979).

The rigid pseudo-atom model reduces the computational effort enormously, but it may easily give unreliable results, especially where charge difference density maps are involved. This can be caused by

relatively small errors in the total density described by the model, which can become relatively large errors in a deformation density map, where the sum of spherical atomic densities is subtracted from the molecular density. Besides that, it is quite difficult to detect which part of the deformation density belongs to one of the pseudo-atoms.

In order to obtain a feasible picture of the effect of internal vibration on a deformation density, we choose to evaluate (1) in a more rigorous computational scheme for diatomic molecules. Here we can use high-quality nuclear wavefunctions and electronic wavefunctions at many different geometries within a reasonable amount of computer time.

The method

In the case of a diatomic molecule we adopt the spin-free vibrating rotator model (Pauling & Wilson, 1935). It should be realized that this model concerns a gas-phase molecule, where temperature effects will depend on the thermal occupation of the vibration-rotation energy levels of a free rotating specimen. Leaving the translations out of consideration, the nuclear motions will be described by the three-dimensional set of polar coordinates \mathbf{R}' .

The electron coordinates \mathbf{r} are defined relative to \mathbf{R}' , with the (internal) z axis coinciding with the internuclear axis \mathbf{R}' . In this coordinate system $\rho(\mathbf{r}; \mathbf{R}')$ is independent of the solid angle Ω' . Now

$$I_n(\mathbf{r}) = \int \psi_n^*(\mathbf{R}') \rho(\mathbf{r}; \mathbf{R}') \psi_n(\mathbf{R}') d\mathbf{R}'. \quad (2)$$

Next we introduce the substitution (Pauling & Wilson, 1935; Schutte, 1976):

$$\psi_n(\mathbf{R}') = \psi_{vJ}(R') Y_{Jm}(\Omega') \frac{1}{R'}, \quad (3)$$

where $Y_{Jm}(\Omega')$ is a spherical harmonic function and v, J are the vibrational and rotational quantum numbers respectively. Integrating over Ω' yields

$$I_{vJ}(\mathbf{r}) = \int \psi_{vJ}(R') \frac{1}{R'} \rho(\mathbf{r}; R') \psi_{vJ}(R') \frac{1}{R'} R'^2 dR'. \quad (4)$$

Using a proper expansion of the vibrational wavefunction $\psi_{vJ}(R')$ in the displacement coordinate $R = R' - R_e$,

$$I_{vJ}(\mathbf{r}) = \int_{-\infty}^{\infty} \rho(\mathbf{r}; R) Q_{vJ}(R\sqrt{\alpha}) \exp(-\alpha R^2) dR, \quad (5)$$

where $Q_{vJ}(R\sqrt{\alpha})$ is the polynomial part of this expansion, which will be discussed in the next section. With $x = R\sqrt{\alpha}$,

$$I_{vJ}(\mathbf{r}) = \frac{1}{\sqrt{\alpha}} \int \rho\left(\mathbf{r}; \frac{x}{\sqrt{\alpha}}\right) Q_{vJ}(x) \exp(-x^2) dx. \quad (6)$$

Now (6) has a suitable form to be evaluated using an accurate numerical integration technique based on a Hermite polynomial (Abramowitz & Stegun, 1964). The integral will be approximated to (with neglect of a small rest term)

$$I_{vJ}(\mathbf{r}) \simeq \frac{1}{\sqrt{\alpha}} \sum \rho\left(\mathbf{r}; \frac{x_i}{\sqrt{\alpha}}\right) Q_{vJ}(x_i) W_i, \quad (7)$$

where the x_i 's are the zeros of the n th order Hermite polynomial on which the integration is based. The weight factors W_i are calculated according to (Abramowitz & Stegun, 1964)

$$W_i = \frac{2^{n-1} n! \sqrt{\pi}}{n^2 [H_{n-1}(x_i)]^2}. \quad (8)$$

Finally, the separate nuclear displacements are found from the relations:

$$R_1 = \frac{\mu}{m_1} R; \quad R_2 = -\frac{\mu}{m_2} R. \quad (9)$$

The vibronic wavefunction

As indicated before, we describe the internal motion of a diatomic molecule by the vibrating rotator model (Pauling & Wilson, 1935; Schutte, 1976). With the substitution of (3) and working out the angular-dependent part, the vibrational wave equation becomes

$$\left[-\frac{1}{2\mu} \frac{d^2}{dR^2} + V(R) + \frac{J(J+1)}{2\mu(R+R_e)^2} \right] \psi_{vJ}(R) = \epsilon_{vJ} \psi_{vJ}(R). \quad (10)$$

Here R is the displacement coordinate (that is, $R = 0$ denotes the equilibrium distance R_e), μ is the reduced mass of the system and $V(R)$ the potential function which will be obtained from the SCF calculations. $V(R)$ can be expanded in a Taylor series in powers of R , where the first-order term vanishes since $V(R)$ has a minimum at $R = 0$. Then a harmonic oscillator approximation is achieved when all terms above second order are neglected and J is put to zero. In this case the vibrational equation becomes

$$\left[-\frac{1}{2\mu} \frac{d^2}{dR^2} + \frac{1}{2} k R^2 \right] \phi_v(R) = \epsilon_v \phi_v(R), \quad (11)$$

where the force constant

$$k \equiv \left[\frac{d^2 V(R)}{dR^2} \right]_{R=0}. \quad (12)$$

Exact solutions of (11) are the orthonormal harmonic oscillator eigenfunctions

$$\varphi_v(R) = N_v H_v(R\sqrt{\alpha}) \exp(-\alpha R^2/2), \quad (13)$$

where v is the vibrational quantum number, $\alpha = \sqrt{\mu k}$, H_v is the v th-order Hermite polynomial and N_v is the normalization constant. The harmonic oscillator eigenfunctions form an appropriate basis for an approximate solution of (10) for low values of v . Thus we expand $\psi_{vj}(R)$ in a linear combination of harmonic oscillator functions:

$$\psi_{vj}(R) = \sum_{i=0}^m a_{vj;i} \varphi_i(R). \quad (14)$$

The coefficients $a_{vj;i}$ in (14) are calculated using the variation method by solving the set of equations

$$\sum_{i=0}^m a_{vj;i} (H_{J;ij} - \varepsilon_{vj} \delta_{ij}) = 0, \quad (15)$$

$$j, v = 0, m,$$

for values of J corresponding to significantly occupied rotational energy levels. In connection with evaluation of matrix elements $H_{J;ij}$ we divide the Hamiltonian in (10) into a harmonic part and two perturbation terms:

$$H_J = -\frac{1}{2} \omega \left(\frac{d^2}{dx^2} - x^2 \right) + V' \left(\frac{x}{\sqrt{\alpha}} \right) + \frac{J(J+1)}{2\mu(x/\sqrt{\alpha} + R_e)^2}, \quad (16)$$

where again $x = R\sqrt{\alpha}$,

$$\omega = \sqrt{k/\mu} \text{ (the harmonic vibration frequency),}$$

and

$$V'(x/\sqrt{\alpha}) = V(x/\sqrt{\alpha}) - \frac{1}{2}k(x/\sqrt{\alpha})^2. \quad (17)$$

Integrals from the first term only give harmonic oscillator energies at the diagonal elements of the H_J matrix, while integrals involving the perturbation term give non-zero contributions for each element of this matrix. Again we have used the Hermite integration technique [cf. (6) and (7)]. This simple method requires only the use of the explicitly calculated potential values $V(x/\sqrt{\alpha})$ in the integration points referred to in (7). These integrals are thus approximated according to:

$$\begin{aligned} & \left\langle \varphi_i \left| V' \left(\frac{x}{\sqrt{\alpha}} \right) + \frac{J(J+1)}{2\mu(x/\sqrt{\alpha} + R_e)^2} \right| \varphi_j \right\rangle \\ & \simeq \frac{1}{\sqrt{\alpha}} N_i N_j \sum_{k=1}^n \left[V' \left(\frac{x_k}{\sqrt{\alpha}} \right) + \frac{J(J+1)}{2\mu(x_k/\sqrt{\alpha} + R_e)^2} \right] \\ & \quad \times H_i(x_k) H_j(x_k) W_k. \end{aligned} \quad (18)$$

The number of harmonic oscillator basis functions in $\psi_{vj}(R)$ was chosen at least one less than the order of

the Hermite polynomial on which both (7) and (18) are based. In a test calculation we applied this integration method to the evaluation of (10) for a model system with a Morse potential and J equal to zero (Johnson, 1977). For the lowest energy levels we obtained an accuracy of at least twelve figures with respect to the exact solution. With the real function $\psi_{vj}(R)$ we infer from (13) and (14) that

$$Q_{vj}(x) = \left[\sum_{i=0}^m a_{vj;i} N_i H_i(x) \right]^2. \quad (19)$$

The eigenvalues ε_{vj} obtained from the solutions of (15) (expressed in the correct dimension) determine the Boltzman weight factors in (1):

$$W_n = W_{vj} = (2J+1) \exp(-\varepsilon_{vj}/kT) \times \left[\sum_{vj} (2J+1) \exp(-\varepsilon_{vj}/kT) \right]^{-1}. \quad (20)$$

The vibrational mean-square amplitude can be obtained for a state v, J by analytical integration:

$$\langle R^2 \rangle_{vj} = \langle \psi_{vj}(R) R^2 \psi_{vj}(R) \rangle. \quad (21)$$

In the harmonic approximation the mean-square amplitude of the zero-point vibration is given by

$$\langle R^2 \rangle_{\text{harm}} = \langle \varphi_0(R) R^2 \varphi_0(R) \rangle = \frac{1}{2\alpha}. \quad (22)$$

At temperature T ,

$$\langle R^2 \rangle_T = \sum_{vj} W_{vj} \langle R^2 \rangle_{vj}, \quad (23)$$

where again W_{vj} are the Boltzman factors from (20).

Results

Using $\Delta\rho = \rho_{\text{mol}} - \sum \rho_{\text{atoms}}$ instead of ρ in the method described above, we performed calculations of the vibrationally averaged deformation density of the diatomics H_2 , BeH , CH , CO and N_2 . In each calculation we made use of LCAO Hartree-Fock-Slater SCF wavefunctions (Baerends & Ros, 1978) in triple- ζ atomic basis sets, extended with a polarization function at each center. For the atomic densities the same method was applied, using an average (spin restricted) configuration.

For the CO and N_2 systems the numerical integration was based on the 21st-order Hermite polynomial, so electronic wavefunctions at 21 internal distances were used. The rather low value of α for the other systems increases the span of the integration points. A high-order H_n leads to large displacements of the nuclei from their equilibrium positions, where the SCF calculations could be less reliable. In order to

obtain a considerable number of integration points in a range of internuclear distances comparable to the CO case, we choose for these systems the 51st-order polynomial, but only used the 23 inner points. These points have weight factors above 10^{-5} and they describe the potential function $V(R)$ up to values of R with positive bond energy in the short distance region. The error due to this truncation in the sum of the weight factors (which equals $\sqrt{\pi}$) is also about 10^{-5} , so the resulting error in the averaged density due to this neglect will be very small: the neglect occurs in the final stage of the calculation [cf. (7)] and limits the accuracy of the averaged density to about four figures.

Another consequence of this approximation is that the potential $V(R)$ in the truncated points will not be known too. Since these values are needed for the calculation of the integrals (18) (and cannot be neglected at this stage in the calculation of the vibronic wavefunction), we estimated them by extrapolation from different exponential series fits of the inner and outer parts of the potential function $V(R)$. At larger displacements errors in these estimates will become larger, but also less important because the weight factors in (18) decrease rather fast to extremely low values.

For each system we started with the calculation of the force constant and equilibrium distance between the nuclei. These values, as given in Table 1, determine the final point distribution. A few spectroscopic constants were obtained from a least-squares fit of the vibration-rotation energy levels in the product expansion of the v, J quantum numbers (Herzberg, 1950; Richards, Raftery & Hinkley, 1974):

$$\varepsilon_{vJ} = \sum_{ij} c_{ij} (v + \frac{1}{2})^i [J(J+1)]^j. \quad (24)$$

The constants ω_e , $\omega_e x_e$, B_e and α_e according to the definitions of Herzberg (1950) are also given in Table 1. Table 2 shows the corresponding experimental values. The calculated values show a good agreement with the experimental ones. This strongly justifies the methodological approach of the evaluation of the vibrational wave equation, and proves the quality of $V(R)$. The theoretical root-mean-square amplitudes are

Table 1. *Calculated equilibrium distances and r.m.s. amplitudes as a fraction of R_e*

	R_e (a.u.)*	Harmonic $v = 0$	100 × r.m.s./ R_e Anharmonic $v = 0, J = 0$	$T = 300$ K
H ₂	1.456	11.70	12.37	12.46
CH	2.172	7.27	7.55	7.61
BeH	2.525	7.18	7.50	7.57
CO	2.132	2.98	3.02	3.02
N ₂	2.047	2.93	2.96	2.97

* 1 a.u. = 0.5292 Å.

given in Table 3, as fractions of the equilibrium distances.

At a temperature of 300 K the contributions of the vibrational ground state and the first excited state are included, each with 15 (for H₂, CH and BeH) or 35 (for CO and N₂) rotational states. The influence upon the r.m.s. amplitudes of this temperature compared to the anharmonic zero-point vibration is quite small. The r.m.s. amplitudes of CO and N₂ are slightly larger than the corresponding values given by Epstein & Stewart (1979).

In Fig. 1 are plotted five deformation densities of CH, calculated at different internuclear distances, contributing to an averaged density calculation based on the fifth-order Hermite polynomial. To obtain this smeared density, each plot should be scaled with the weight factor which belongs to that displacement, these results should then be summed and finally the sum

Table 2. *Calculated spectroscopic constants (in cm⁻¹)*

	ω_e	$\omega_e x_e$	B_e	α_e
H ₂	4120	112	56.3	2.67
CH	2616	49	13.8	0.49
BeH	2030	43	10.5	0.39
CO	2174	13	1.93	0.017
N ₂	2390	14	2.05	0.018

Table 3. *Experimental spectroscopic constants (in cm⁻¹)*

[See Herzberg (1950), Mills (1974), Baerends & Ros (1978).]

	ω_e	$\omega_e x_e$	B_e	α_e
H ₂	4403	121.6	60.9	2.99
CH	2859	63.3	14.4	0.53
BeH	2059	35.5	10.3	0.30
CO	2170	13.3	1.93	0.0175
N ₂	2358	14.2	2.00	0.0187

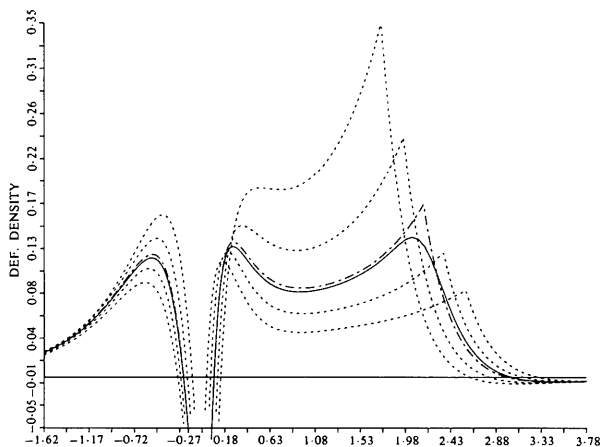


Fig. 1. Deformation densities in CH: ——— static, equilibrium distance; - - - - static at four displacements (cf. Table 4); ····· dynamic.

normalized. [These weightfactors including the polynomial contributions $Q(R\sqrt{\alpha})$ from the harmonic and anharmonic vibrational wave functions are given in Table 4.]

The averaged density plotted in Fig. 1 is the accurate one, consisting of 23 anharmonic (with $v = 0, J = 0$) weighted contributions. This figure shows that the vibrationally averaged deformation density lies close to the static one at equilibrium distance, which could be regarded as a consequence of decreasing weight factors at increasing displacements. If harmonic weight factors were used, the resulting smeared deformation density in the bond region would be found at about the same distance above the static density as the anharmonic-weighted one was found below it.

In Figs. 2, 3 and 4 are plotted in the y - z halfplane, respectively the static and dynamic deformation densities of BeH and the difference between them (the latter with lower contour values). From these figures it is obvious that the averaging of the deformation density due to the internal vibration is very small, even in systems with a low value of α . The resemblance between our results and those of Becker (1977, Fig. 25a) for the BeH molecule is small, which is mainly

Table 4. Displacements and weight factors for CH as obtained from calculations based on the fifth-order Hermite polynomial

Displacement (a.u.)	Weight factors		
	Harmonic $v = 0$	Anharmonic $v = 0, J = 0$	$T = 300$ K
0.4555	0.01995	0.05065	0.05371
0.2161	0.3936	0.5016	0.5144
0.0000	0.9453	0.9273	0.9221
-0.2161	0.3936	0.2869	0.2766
-0.4555	0.01995	0.006007	0.005582

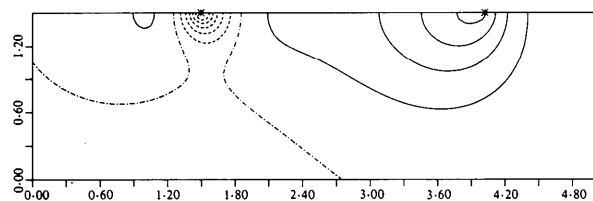


Fig. 2. Static deformation density in BeH. Contours at 0.0, 0.03, 0.06, 0.09, 0.12, 0.15 e (a.u.)⁻³ (negative contours dotted lines).

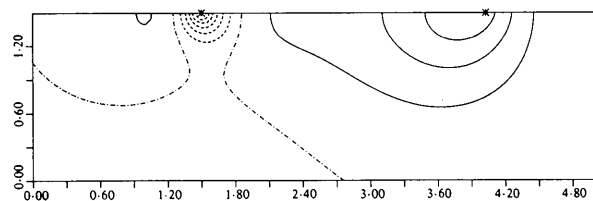


Fig. 3. Dynamic deformation density in BeH. Same contours as in Fig. 2.

because Fig. 4 represents the difference between deformation densities, while Becker shows the corresponding difference between total densities.

Both the static and smeared deformation densities of CO along the internuclear axis are plotted in Fig. 5. Except at sharp peaks in the deformation density, the effect of vibrational smearing turns out to be negligible. For the N₂ system our calculation led to the same result as for the CO system.

Like Coulson & Thomas (1971) we calculated the apparent bond lengths of the hydrogen molecule. For various vibronic wavefunctions the bond shortening referred to R_e was 6.05% [harmonic approximation, compare with 5.71% of Coulson & Thomas (1971)], 3.02% (anharmonic zero-point vibration) and 1.92% ($T = 300$ K).

Discussion and conclusions

(1) From the results presented above it will be clear that in each system we investigated, the vibrationally averaged deformation density cannot be regarded as considerably different from the static one at equilibrium distance [cf. Thomas (1973) for calculations with H₂⁺]. At 300 K the temperature influence upon this smearing of the deformation density is negligible compared to the results obtained with the anharmonic zero-point vibration. Since the main effect is described by pure

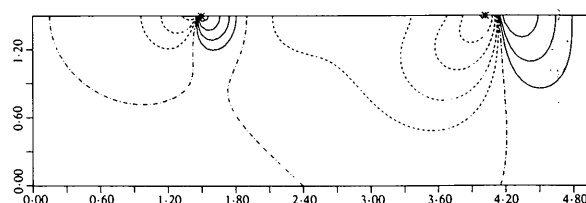


Fig. 4. Difference between static (Fig. 2) and dynamic (Fig. 3) deformation density in BeH. Contours at 0.0, 0.001, 0.002, 0.004, 0.008, 0.02 e (a.u.)⁻³.

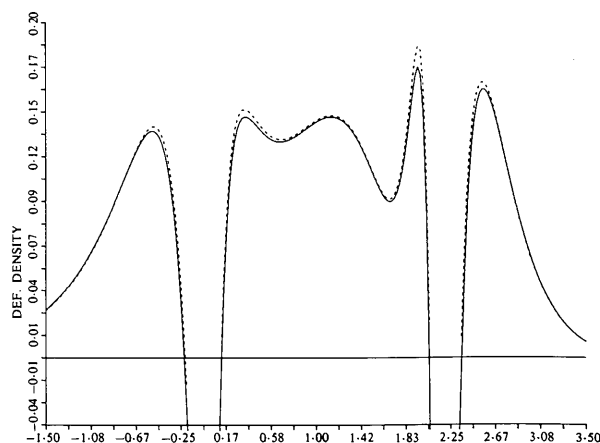


Fig. 5. Deformation density in CO: ----- static; ———— dynamic.

vibration, the rotation can be deleted from the initial model. This simplifies an extrapolation to the influence of an isolated internal vibration in a molecular crystal.

(2) Within the Born–Oppenheimer approximation (which includes the separation of the electronic and vibronic Schrödinger equations) the method used in these calculations will be correct. It will be possible to increase the accuracy by taking more integration points (using a higher-order H_n), but even then we do not expect other results, since test calculations with fewer points showed the same effect of this smearing as the results presented here.

(3) We do not expect other results than those found here, if more accurate electronic wavefunctions are used. The vibrational smearing within this model is a consequence of changes in the static deformation density at different displacements of the nuclei, and not of the deformation density itself. We note that it has been shown (Baerends & Ros, 1978; Heijser, van Kessel & Baerends, 1976; de With & Feil, 1975) that the deformation density calculated with HFS–SCF wavefunctions at equilibrium distance is quite reasonable. If differences with higher quality wavefunctions at larger displacements should become larger, this does not play an important role due to the decreasing weight factors.

(4) With both harmonic and anharmonic vibrational wavefunctions used for the calculation of the averaged deformation density, the absolute values of the difference with the static density were of the same size, but the sign of the difference between the static and harmonic averaged density may be opposite to the sign of the difference between the static and anharmonic averaged density. The plotted results presented above are calculated with the anharmonic zero-point vibrational wave function.

(5) The effect of including temperature was small for both the r.m.s. amplitudes and the averaged deformation densities in the bond region. The apparent bond length of hydrogen shows a more significant temperature dependence. Thus, for this smearing the anharmonic zero-point vibration is a very good approximation for these molecules. This is also seen from the weight factors in Table 4, the introduced asymmetry between inner and outer contributions is only slightly affected by including temperature.

(6) The deconvolution of experimentally obtained deformation densities of systems similar to those mentioned here (in order to obtain a better comparison with a static theoretical density) is not necessary. For example, in the N_2 case [*cf.* Fink *et al.* (1976) for an experimental result with deconvolution] we calculated the averaged deformation density in the center of the bond to be about 0.5% lower than the static density. This difference is much smaller than the accuracy of any density calculated with an SCF method (Baerends & Ros, 1978; Smith, 1980).

In future investigations we will pay attention to the application of this method to the bending mode vibration of triatomics (*e.g.* the water molecule), and on the other hand to the application of the numerical integration technique to rigid-body motions of larger molecules. The latter case has the disadvantage of needing experimentally determined mean-square displacements, since it will be practically impossible to calculate a force field for the external motions.

This investigation was supported in part by the Netherlands Organization for Chemical Research (SON) with financial aid from the Netherlands Organization for the Advancement of Pure Research (ZWO).

References

- ABRAMOWITZ, M. & STEGUN, A. (1964). Editors. *Handbook of Mathematical Functions*. Washington: National Bureau of Standards.
- BAERENDS, E. J. & ROS, P. (1978). *Int. J. Quant. Chem.* **12**, 169–190.
- BECKER, P. (1977). *Phys. Scr.* **15**, 119–142.
- COPPENS, P. & STEVENS, E. D. (1977). In *Advances in Quantum Chemistry X*, edited by P. LÖWDIN. New York: Academic Press.
- COULSON, C. A. & THOMAS, M. W. (1971). *Acta Cryst.* **B27**, 1354–1359.
- EPSTEIN, J., STEWART, R. F. (1979). *Acta Cryst.* **A35**, 476–481.
- FEIL, D. (1977). *Isr. J. Chem.* **16**, 149–153.
- FINK, M., GREGORY, D. & MOORE, P. G. (1976). *Phys. Rev. Lett.* **37**, 15–18.
- HEIJSER, W., VAN KESSEL, A. TH. & BAERENDS, E. J. (1976). *Chem. Phys.* **16**, 371–379.
- HERZBERG, G. (1950). *Molecular Spectra and Molecular Structure I*. New York: Van Nostrand.
- HIRSHFELD, F. L. (1976). *Acta Cryst.* **A32**, 239–244.
- HIRSHFELD, F. L. (1977). *Isr. J. Chem.* **16**, 168–174.
- JOHNSON, B. R. (1977). *J. Chem. Phys.* **67**, 4086–4093.
- MILLS, I. M. (1974). In *Theoretical Chemistry*, Vol. I, edited by R. N. DIXON. London: The Chemical Society.
- PAULING, L. & WILSON, E. B. (1935). *Introduction to Quantum Mechanics*. New York: McGraw Hill.
- RICHARDS, W. G., RAFTERY, J. & HINKLEY, R. K. (1974). In *Theoretical Chemistry*, Vol. I, edited by R. N. DIXON. London: The Chemical Society.
- RUYSINK, A. F. J. & VOS, A. (1974). *Acta Cryst.* **A30**, 497–502.
- SCHUTTE, C. J. H. (1976). *The Theory of Molecular Spectroscopy*, Vol. I. Amsterdam: North-Holland.
- SMITH, V. H. JR (1980). In *Electron and Magnetization Densities in Molecules and Crystals*, edited by P. BECKER. New York: Plenum Press.
- SMITH, V. H. JR & ABSAR, I. (1977). *Isr. J. Chem.* **16**, 87–102.
- STEVENS, E. D., RYS, J. & COPPENS, P. (1977). *Acta Cryst.* **A33**, 333–338.
- STEWART, R. F. (1977). *Isr. J. Chem.* **16**, 137–143.
- THOMAS, M. W. (1973). *Chem. Phys. Lett.* **20**, 303–305.
- WITH, G. DE & FEIL, D. (1975). *Chem. Phys. Lett.* **30**, 279–283.